Journal of Applied Polymer Science

Emulsion Polymerization of Isoprene: Mathematical Model for Long-Chain Branching

Virginia I. Rodríguez, Roque J. Minari, Diana A. Estenoz, Luis M. Gugliotta, Gregorio R. Meira
INTEC, Universidad Nacional del Litoral-CONICET, Güemes 3450, Santa Fe 3000, Argentina
Correspondence to: G. R. Meira (E-mail: gmeira@santafe-conicet.gov.ar)

ABSTRACT: For a batch emulsion polymerization of isoprene at 10°C in the presence of a chain transfer agent, a previous mathematical model (Minari et al., J. Appl. Polym. Sci. 2010, 116, 590) was extended for predicting the molecular weight distributions of all the generated long chain branched topologies; with each topology characterized by the number of tri- and tetra-functional branches per molecule. According to the new model predictions, at the reaction end the linear topology remains as the most abundant (with ∼ 40% of the total mass), followed by the single trifunctionally branched topology (with ∼ 20% of the total mass). The model can be used for developing strategies for controlling the distribution of branches/molecule, for estimating melt viscosities, etc.
© 2012 Wiley Periodicals, Inc. J. Appl. Polym. Sci. 127: 1038–1046, 2013

KEYWORDS: polyisoprene; emulsion polymerization; molecular weight distribution; long-chain branching

Received 9 July 2011; accepted 9 March 2012; published online 10 May 2012
DOI: 10.1002/app.37658

INTRODUCTION

Chain branching is present in many important synthetic polymers such as polyethylenes and polyacrylates. In radical polymerization, short-chain branching is produced by intramolecular transfer to the polymer, whereas long-chain branching is produced by intermolecular chain transfer to the polymer. Short-chain branching affects the melting point, glass-transition temperature, hardness, and degree of crystallinity. Long-chain branching affects rheological properties such as sedimentation behavior, intrinsic viscosity, and the viscosity and elasticity of a polymer melt. ^{13}C nuclear magnetic resonance (NMR) spectroscopy is the main absolute technique for measuring average branching. With this technique, branching frequencies of up to a few percents of monomer units have been determined for a poly(*n*-butyl acrylate) synthesized by emulsion polymerization.[1] Recently, the alternative approach of melt-state, high-resolution magic angle spinning NMR has enabled to determine degrees of branching as low as 0.001% of monomer units in 1 day, for sparsely branched polyolefins.[2] Unfortunately, no analytical technique is so far capable of fractionating molecules according to their number of long chain branches, and therefore no quantitative methods are available for determining the distribution of long chain branches/molecule (LCBD). However, and with many limitations, semi-quantitative estimates of such distribution are indirectly determined by size exclusion chromatography fitted with molar mass sensitive detectors.[3,4]

The molecular characteristics of a diene rubber affect its processability, vulcanization behaviour, and properties of the cured material. These molecular characteristics include the distribution of molecular weights (MWD), the LCBD, and the contents and distributions of the various repeating unit types. Commercial synthetic polyisoprenes are mostly linear, and aim at maximizing the 1,4-*cis* content. Thus, commercial Ziegler-Natta and anionic polyisoprenes respectively contain ∼ 96% and 90% of 1,4-*cis* isomer. In contrast, radical polyisoprenes are branched and contain mixtures of 1,4-*trans*, 1,4-*cis*, 1,2 vinyl, and 3,4 vinyl units. The branches are mainly trifunctional (obtained by chain transfer reactions to the accumulated polymer) and also tetrafunctional (obtained by propagation with internal double bonds). With excessive branching, the base rubber becomes an insoluble gel.[5] In radical emulsion polymerizations, the molecular weights and degrees of branching are typically controlled by addition of a chain transfer agent (CTA), and/or by limiting the monomer conversion to ∼ 80%.

Emulsion polymerizations are complex processes, due to the heterogeneous nature of the reaction mechanism, and to the partition of reagents and products between the phases. For example, while long-chained radicals cannot be normally desorbed from the polymer particles, some short-chain CTA radicals can be both absorbed and desorbed. Also, propagation and termination reactions can occur simultaneously in the aqueous and polymer phases.

© 2012 Wiley Periodicals, Inc.

Table I. Emulsion Polymerization of Isoprene: Global kinetics by Minari et al.[4]

	Polymer phase (n, m = 1, 2,...)	Aqueous phase (n, m = 1, 2,...)
Initiation	—	$I + Fe^{2+} \xrightarrow{k_1} R_c^{\cdot} + Fe^{3+} + OH^-$ $Fe^{3+} + Ra \xrightarrow{k_2} Fe^{2+} + Ra^+$ $R_c^{\cdot} + Is \xrightarrow{k_{pc}} R_{(1)_w}^{\cdot}$
Reinitiation	$Is^{\cdot} + Is \xrightarrow{k_{pI}} R_{(2)}^{\cdot}$ $X^{\cdot} + Is \xrightarrow{k_{pX}} R_{(2)}^{\cdot}$	—
Propagation to the monomer	$R_{(n)}^{\cdot} + Is \xrightarrow{k_p} R_{(n+1)}^{\cdot} \quad n \geq 2$	$R_{(n)_w}^{\cdot} + Is \xrightarrow{k_{pw}} R_{(n+1)_w}^{\cdot}$
Termination reactions	$R_{(n)}^{\cdot} + R_{(m)}^{\cdot} \xrightarrow{k_{tp}} P(n,m)$ $R_{(n)}^{\cdot} + R_{(m)}^{\cdot} \xrightarrow{k_{tp}} P(n) + P(m)$	—
Chain transfer to the monomer	$R_{(n)}^{\cdot} + Is \xrightarrow{k_{fM}} P(n) + Is^{\cdot}$	—
Chain transfer to the CTA	$R_{(n)}^{\cdot} + X \xrightarrow{k_{fX}} P(n) + X^{\cdot}$	—
Chain transfer to the polymer	$R_{(n)}^{\cdot} + P(m) \xrightarrow{k_{fP}} P(n) + R_{(m)}^{\cdot}$	—
Propagation with an internal double bond	$R_{(n)}^{\cdot} + P(m) \xrightarrow{k_p^*} R_{(n+m)}^{\cdot}$	—

I, Is, and X are, respectively, the initiator, the monomer, and the CTA; Fe^{2+} is a ferrous ion introduced with the $FeSO_4$ salt; Ra is a reducing agent; $R_c^{\cdot}$ is a primary initiator radical; $R_{(1)w}^{\cdot}$ and $Is^{\cdot}$ (equivalent to $R_{(1)}^{\cdot}$) are primary monomer radicals in the aqueous and polymer phases, respectively; $X^{\cdot}$ is a primary CTA radical; $R_{(n)w}^{\cdot}$ and $R_{(n)}^{\cdot}$ are free-radicals with n repetitive units in the aqueous and polymer phases, respectively; and P(n) is a dead polymer molecule in the polymer phase containing n repetitive units.

Emulsion polymerization models have been classified according to the adopted assumptions on the compartmentalization of radicals in the polymer particles.[6] The simplest pseudo-bulk models calculate the MWDs as in a bulk process[4,7–10]; with the total concentration of radicals estimated from the product between the total number of latex particles and the average number of radicals per particle. Pseudo-bulk models have proven adequate for emulsion systems where of the dead polymer is mostly generated in the polymer phase by chain transfer reactions (to the CTA and to the polymer).[6,7] Semi-compartmentalized models[11,12] assume a random distribution of radicals among the particles. Partial distinction models subdivide the population of radicals into shorter radicals (that can be transferred between the phases) and longer radicals (that cannot escape from the polymer particles).[13–16] The most sophisticated models assume a distribution of radical chain lengths among the polymer particles, that in turn can be either mono- or polydisperse in diameter.[17–27] Several algorithms have been developed for the numerical resolution of the mentioned models: method of moments,[4,6,7,9,10] orthogonal collocation on finite elements,[12] numerical fractionation,[13–16,18,19] Markov chains,[22] and Monte-Carlo simulations.[24–27]

Several models have been developed that calculate the long-chain branching characteristics of emulsion polymers. For an acrylonitrile–butadiene rubber, the model by Rodriguez et al.[8] predicts the bivariate distribution of chain lengths and composition for each of the generated branched topologies; without distinguishing between tri- and tetra-functional branches. For a seeded and semibatch emulsion polymerization of *n*-butylacrylate, the model by Plessis et al.[13] considers the development of long- and short-chain branches, and calculates the MWD of the sol fraction, the amount of gel, and the global branching frequency. For a generalized emulsion polymerization, Ghielmi et al.[18] employed a numerical fractionation technique for modeling the MWD of a long-chain-branched polymer. Similarly, Butte et al.[20] developed a general model for long-chain-branched emulsion polymers. It calculates an approximate MWD by partitioning the overall population of molecules into classes according to the number of branches per molecule. Tobita[25] developed a general model for predicting the global MWD of a branched polymer generated by chain transfer to the polymer; claiming that the conventional method of moments provides good estimates for the less branched fraction, but overestimates the weight–average chain lengths of the more highly branched fraction. For an emulsion polymerization of butadiene, Jabbari[26] employed a Monte-Carlo technique for simulating the effects of trifunctional branching and tetrafunctional cross-linking on the MWD. According to that model, both branching

Table II. Batch Emulsion Polymerization at 10°C and Stirring Rate 250 rpm: Recipe and Final Global Characteristics of Experiment 1 (reproduced from Minari et al.[4])

Recipe (in pphm[a])		
Monomer (isoprene, Is)	100	
CTA (*n*DM)	1.55	
Initiator (PMHP)	0.073	
Oxidant ($FeSO_4.7H_2O$)	0.034	
Reducing agent (SFS)	0.10	
Buffer (EDTA)	0.09	
Emulsifier (SLS)	11.76	
Water	399.9	
Final Polymer Characteristics	Measurements	Simulated Results
Monomer conversion (%)	84.6	82.6
$\overline{M}_n$ (g/mol)	25,400	37,700
$\overline{M}_w$ (g/mol)	262,000	298,000
$\overline{M}_w/\overline{M}_n$	10.3	7.9
$\overline{B}_{n3}$ (molecule^{-1})	0.32	0.37

[a]Parts per hundred monomer.

types increase linearly with conversion, yielding a bimodal MWD. Arzamendi and Leiza[27] modeled a semibatch emulsion polymerization of acrylate monomers. The model calculates the following: (a) the MWD of the sol fraction through a Monte-Carlo algorithm that includes the production of short-chain branching by backbiting; (b) the production of long-chain branching by chain-transfer to the polymer; and (c) the generation of ultra-high molecular weight by recombination termination.

This article extends the mathematical model by Minari et al.,[4] with the aim of predicting the detailed long chain branching characteristics of an emulsion polyisoprene. The extended model predicts the MWDs of all the generated branched topologies, with each topology characterized by the number of tri- and tetra-functional branches per molecule.

EXTENDED MODEL

Minari et al.[4] investigated an emulsion polymerization of isoprene at 10°C and the following reagents: *p*-menthane hydroperoxide (PMHP) as redox initiator, $FeSO_4$ as oxidant agent, sodium formaldehyde sulfoxilate (SFS) as reducing agent, ethylenediaminetetraacetic acid (EDTA) as buffer, sodium lauryl sulphate (SLS) as emulsifier, and *n*-dodecyl mercaptan (nDM) as chain transfer agent (CTA). Three polymerizations were carried out, with recipes that differed in the initial CTA concentration. A mathematical model of the process was developed on the basis of a kinetic mechanism that considers reactions in the aqueous and polymer phases[28] (Table I). It assumes absence of oxygen or other impurities, and neglects termination in the aqueous phase. The following assumptions were also adopted: (a) polymer particles are generated by micellar nucleation; (b) the particle size distribution is monodisperse; (c) radicals are in a pseudo-stationary state; (d) reagents are distributed between the phases according to constant partition coefficients; (e) CTA radicals can desorb from the polymer particles; (f) volume changes due to mixing are negligible; (g) monomer consumption by transfer or initiation reactions is negligible (long chain approximation); and (h) a negligible amount of polymer is produced in the water phase. In addition, the MWD and average branching are calculated through a reduced reaction mechanism in the polymer phase that neglects termination reactions, and only considers reinitiation, propagation to the monomer, chain

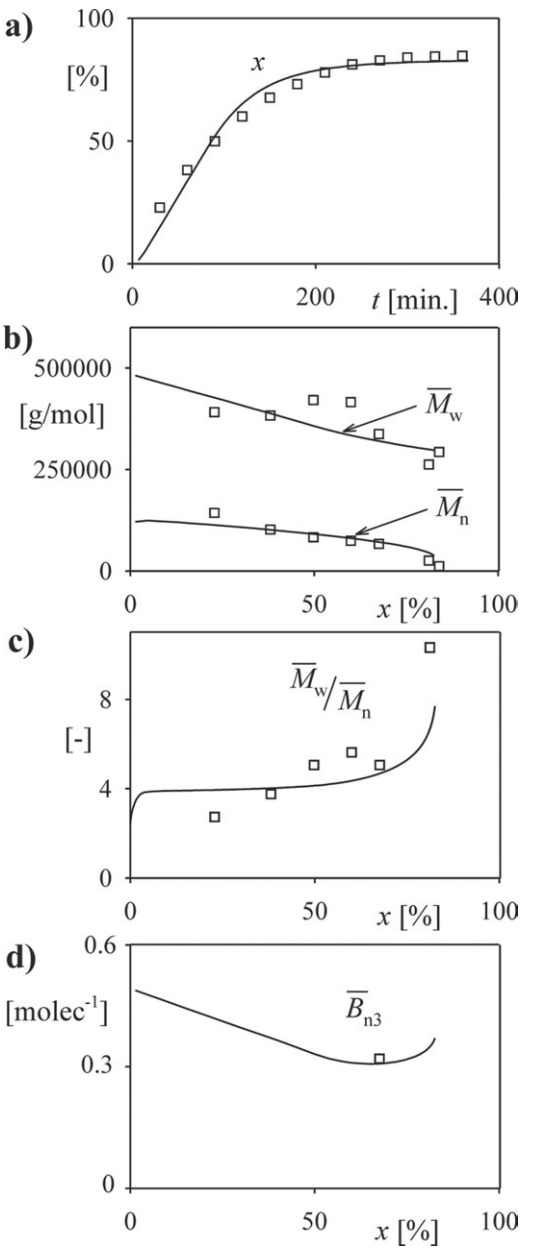

Figure 1. Measurements and model predictions in Experiment 1 for: (a) monomer conversion (x); (b) average molecular weights ($\overline{M}_w$, $\overline{M}_n$); (c) dispersity ($\overline{M}_w/\overline{M}_n$); and (d) number–average number of trifunctional branches per molecule ($\overline{B}_{n3}$) (From Minari et al.[4])

Table III. Polymerization of Isoprene at 10°C: Kinetic Constants (Reproduced from Minari et al.[4])

Parameter	Value ($dm^3\ mol^{-1}\ min^{-1}$)	Reference
$k_p = k_{pX} = k_{pI}$	1.94×10^2	Morton et al.[33]
k_{fM}	3.47×10^{-2}	Minari et al.[4]
k_{fX}	1.032×10^1	Minari et al.[4]
k_{fP}	5.36×10^{-2} [a]	Minari et al.[4]
k_p^*	6.93×10^{-10}	Minari et al.[4]

[a]Value for Experiment 1,[4] as adjusted from the final measurement of $\overline{M}_w$.

transfer to the monomer, chain transfer to the CTA, chain transfer to the polymer, and propagation with internal double bonds of the accumulated polymer. Despite its limitations, this class of model has proven successful for predicting the base molecular structure of branched emulsion polymers such as polyacrylates[29] and butadiene rubbers.[7,30] In addition, it has been applied onto miniemulsion systems containing hydrophobic components in the polymer particles.[31,32]

In this work, Experiment 1 of Minari et al.[4] is reconsidered. The recipe is presented in the upper section of Table II. The measurements and model predictions for conversion, average molecular weights, and number–average number of trifunctional branches per molecule are reproduced in Figure 1 and Table II (*Final Polymer Characteristics*). As expected, the average molecular weights were strongly affected when varying the initial CTA concentration. In contrast, the monomer conversion and the number–average number of trifunctional branches per molecule ($\overline{B}_{n3}$) proved both quite insensitive to the initial CTA concentration. This insensitivity of $\overline{B}_{n3}$ toward the CTA was attributed to a diffusion-control effect in the chain transfer reactions to the polymer; and such effect was modeled by imposing a linear correlation between the rate constant of chain transfer to the polymer (k_{fP}) and the $\overline{M}_w$ measurements.[4] The model parameters are presented in Table III. The ratio between the rate of chain transfer to the CTA and the rate of propagation ($C_X = k_{fX}/k_p \approx 0.05$) is much lower than unity (Table III). For this reason, the concentration ratio between CTA and monomer in the polymer particles steadily increases. This, in turn reduces the chain lengths of the newly generated chains and branches, and reduces the values of $\overline{B}_{n3}$ up to around 68% conversion, when it attains a minimum.

The new Macromolecular Structure Module (Appendix) adopts the simulation results from Minari et al.[4] as inputs for calculating the MWDs of each generated branched topology. The inputs to the new model (monomer conversion, phase volumes, and concentrations of reagents and products in the polymer phase) were all estimated through the base model by Minari et al.[4] Except for the termination reactions, the reaction mechanism of Table I in the polymer phase was rewritten (Table IV); to identify each of the generated molecular species according to their chain length and number of branches. The approach is similar to that applied in Estenoz et al.[34] for the grafting of polybutadiene in a bulk high-impact polystyrene process. The model extension assumes that (irrespective of the microstructure), all the isoprene units exhibit equal reactivities towards branching. Each topology is characterized by the number of tri- and tetrafunctional branches per molecule; respectively represented by the non-negative integers c and d.

Appendix presents the extended mass balances for reagents and products. In particular, eqs. (A3)–(A9) represent the molar balances for every possible radical and polymer species. The computer program was written in Fortran Power Station 4.0. The base model by Minari et al.[4] was solved with an integration routine appropriate for stiff numerical systems. The model extension was solved with a finite difference method that used as inputs the outputs of Minari et al.[4] at fixed time intervals: $\Delta t = 30$ s. Also, the total number of molecular species was reduced by lumping together species of similar chain lengths into single hypothetical species. More specifically, fixed chain length intervals $\Delta n = 50$ were adopted for the MWDs of every molecular topology. To ensure a wide enough range of molecular weights, an upper molecular weight limit of 1.08×10^7 g/mole was selected. This value is 30 times larger than the final measurement of $\overline{M}_w$. Through this approach, each generated topology was characterized by a chain length distribution of 3200 hypothetical chain lengths. All the possible topologies with $c = 0, 1, 2, \ldots, 50$ trifunctional branches and $d = 0, 1, 2$ tetrafunctional branches were *a priori* assumed. However, the simulations by Minari et al.[4] had predicted a negligible amount of tetrafunctional branching points; and this was confirmed by the new results, where less than 0.1% in weight of the final polymer exhibited a single tetrafunctional branching point. For this reason, tetrafunctional branching was neglected, and the topologies were directly identified by the number of trifunctional branches

Table IV. Detailed Kinetics in the Polymer Phase of the New Macromolecular Structure Module; with ($a, b, c, d, m = 0, 1, 2, \ldots$) and ($n, p = 1, 2, \ldots$)

Reinitiation	$Is^{\cdot} + Is \xrightarrow{k_{pI}} R^{\cdot}_{(2)}(0)_{0,0}$ $X^{\cdot} + Is \xrightarrow{k_{pX}} R^{\cdot}_{(2)}(0)_{0,0}$
Propagation to the monomer	$R^{\cdot}_{(n)}(m)_{a,b} + Is \xrightarrow{k_p} R^{\cdot}_{(n+1)}(m)_{a,b} \geq 2$
Chain transfer to the monomer	$R^{\cdot}_{(n)}(m)_{a,b} + Is \xrightarrow{k_{fM}} P(n+m)_{a,b} + Is^{\cdot}$
Chain transfer to the CTA	$R^{\cdot}_{(n)}(m)_{a,b} + X \xrightarrow{k_{fX}} P(n+m)_{a,b} + X^{\cdot}$
Chain transfer to the polymer	$R^{\cdot}_{(n)}(m)_{a,b} + P(p)_{c,d} \xrightarrow{k_{fP}} P(n+m)_{a,b} + R^{\cdot}_{(0)}(p)_{c+1,d}$
Propagation with an internal double bond	$R^{\cdot}_{(n)}(m)_{a,b} + P(p)_{c,d} \xrightarrow{k_p^*} R^{\cdot}_{(0)}(n+m+p)_{a+c,b+d+1}$

$P(p)_{c,d}$ is a polymer molecule of topology (c, d) with p repetitive units; $R^{\cdot}_{(0)}(p)_{c,d}$ is a primary polymer radical generated by chain transfer to the polymer or by propagation with an internal double bond; and $R^{\cdot}_{(n)}(p)_{c,d}$ is a non-primary radical with a new growing chain of n repetitive units, generated from $R^{\cdot}_{(0)}(p)_{c,d}$. In particular, $R^{\cdot}_{(n)}(0)_{0,0}$ is a linear radical. Note that $Is^{\cdot}$ is equivalent to $R^{\cdot}_{(1)}(0)_{0,0}$.

Applied Polymer SCIENCE

Table V. Polymerization of Isoprene at 10°C. Model Predictions for the Mass Fractions and Average Molecular Weights of the Generated Topologies in Experiment 1 at 82.6% Conversion.

Number of trifunctional branches/ molecule (c)	Mass fraction (%)	$\overline{M}_n$ (g/mol)	$\overline{M}_w$ (g/mol)	$\overline{M}_w/\overline{M}_n$
0	40.72	13,863	40,380	2.91
1	20.77	56,959	94,578	1.66
2	11.51	110,108	148,181	1.35
3	7.20	164,943	202,776	1.23
4	4.87	221,107	258,545	1.17
5	3.46	278,063	315,010	1.13
6	2.44	335,238	371,683	1.11
7	1.82	392,266	428,253	1.09
8	1.39	448,980	484,577	1.08
9	1.08	505,329	540,605	1.07
10	0.86	561,324	596,339	1.06
11	0.69	616,993	651,801	1.06
12	0.56	672,368	707,032	1.05
13	0.46	727,501	762,128	1.05
14	0.38	782,411	817,238	1.04
15	0.32	837,172	872,773	1.04
16	0.27	891,953	929,275	1.04
17	0.23	946,855	987,378	1.04
18	0.20	1,002,043	1,047,497	1.05
19	0.17	1,057,556	1,109,432	1.05
20	0.14	1,113,320	1,172,343	1.05
21	0.11	1,169,546	1,237,073	1.06
22	0.09	1,226,605	1,304,867	1.06
23	0.07	1,284,816	1,376,272	1.07
24	0.05	1,344,494	1,451,751	1.08
25	0.03	1,405,969	1,531,699	1.09
26	0.01	1,469,644	1,616,268	1.10
:	:	:	:	:
50	9.6×10^{-4}	2,988,544	3,107,934	1.04
Total polymer	100	37,695	297,632	7.896

per molecule (c). As expected, a negligible mass fraction of the highest admissible topology ($c = 50$) was observed at the reaction end (Table V).

DISCUSSION

The new model predictions are presented in Table V and in Figures 2–5. Before analyzing the new results, it was verified that the global averages calculated from the MWDs of all the generated topologies, coincided with the original predictions of Figure 1.

Table V presents the mass fractions and average molecular weights of each estimated topology at 82.6% conversion. At that conversion, the linear topology remains as the most abundant (representing ~ 40% of the total mass), followed by the single trifunctional-branched topology (~ 20% of the total mass). The higher topologies exhibit the higher average molecular weights and the lower dispersities. These low dispersities are a consequence of compensation between the longer and shorter branches. Finally, note the rather large dispersity of the final total polymer (Table V); because it combines the lower molecular weights of the linear fraction and the higher molecular weights of the highly branched fractions.

For the total polymer and main topologies, Figure 2 presents the evolution of the masses and average molecular characteristics vs. the monomer conversion. As expected, the total polymer mass increases linearly with conversion. The linear topology (of

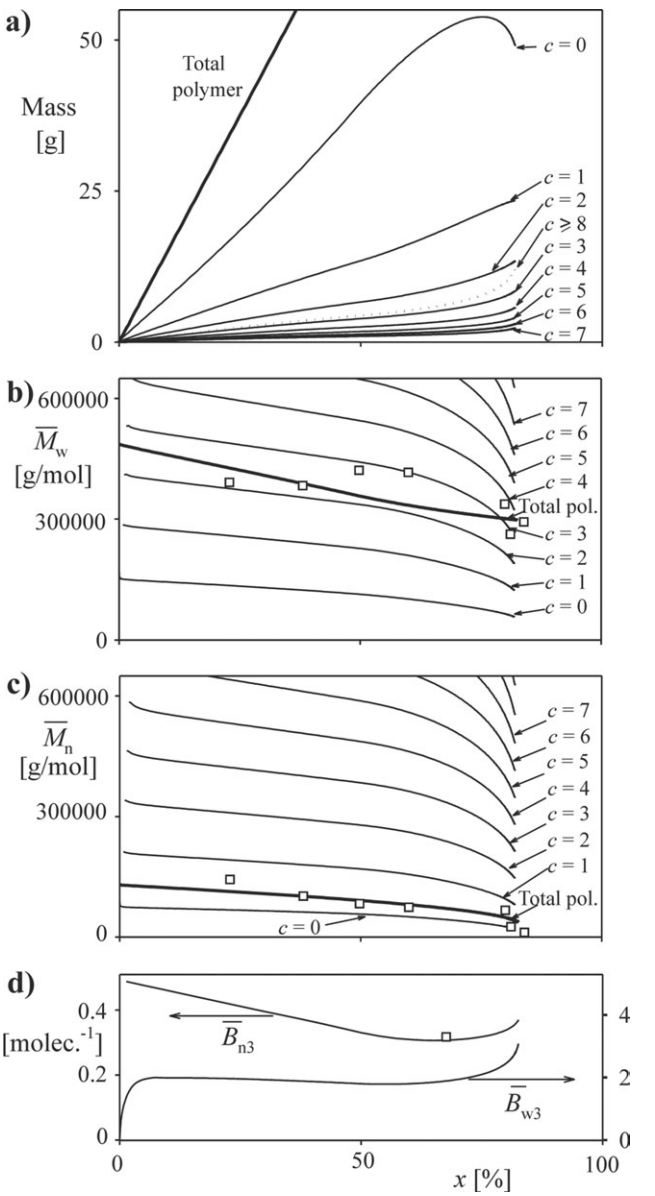

Figure 2. Model predictions *vs.* conversion in Experiment 1 for: (a) mass of total polymer and main topologies; (b, c) average molecular weights of total polymer and main topologies; and (d) global number– and weight–average number of trifunctional branches per molecule ($\overline{B}_{n3}$ and $\overline{B}_{w3}$, respectively).

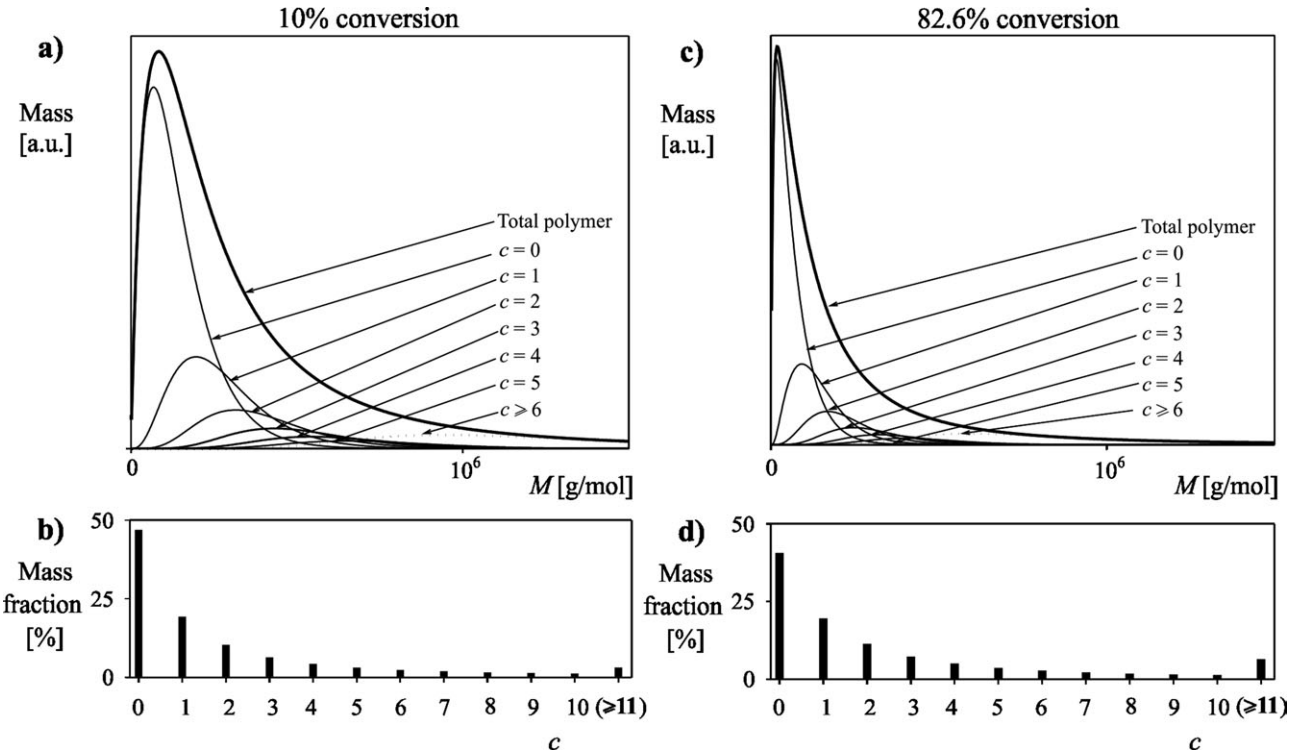

Figure 3. Model predictions for the MWDs and LCBDs in Experiment 1 at conversions of 10% (a, b), and 82.6% (c, d). The corresponding averages at 82.6% conversion are given in Table V.

$c = 0$) remains as the most abundant throughout the reaction, but it decreases after $\sim$ 75% conversion, are totally consumed. The final decrease in the mass of linear topology is due to an increased rate of branching relative to generation of new (linear) molecules. This occurs after disappearance of the monomer droplets, as a consequence of an increased concentration of polymer relative to monomer in the polymer particles [Figure 1(d)]. For all the topologies, their masses increase monotonically with conversion. In addition, the average molecular weights of all the topologies and total polymer decrease monotonically with conversion [Figure 2(b,c)]. This drop is caused by accumulation of CTA with respect to the monomer in the polymer particles; that overcomes the increased rate of branching after disappearence of the monomer droplets. The linear topology continuously reduces its average molecular weights for the mentioned accumulation of CTA relative to monomer, and for the higher probability of branching of the longer chains with respect to the shorter.

In addition to reestimating the evolution of $\overline{B}_{n3}$ [Figures 1(d) and 2(d)], the extended model also enables the calculation of the weight–average number of trifunctional branches per molecule ($\overline{B}_{w3}$). Note that while $\overline{B}_{n3}(x)$ falls along most of the polymerization, $\overline{B}_{w3}(x)$ remains essentially constant until a final rise observed after 75% conversion, when the monomer droplets are totally depleted [Figure 2(d)]. The final value of $\overline{B}_{n3}$ ($\approx$0.35 branches/molecule) could be in principle considered as a low degree of branching. Note however, the considerably higher value of the corresponding weight average $\overline{B}_{w3}$ ($\approx$3 branches/molecule). These averages correspond to an average branching frequency of around 0.03 branching points per 100 repeating units. Unfortunately, this value is too low for its experimental validation by standard ^{13}C-NMR.[35]

Figure 3 presents the distributions of molecular weights and number of branches/molecule, at 10% and 82.6% conversion. In Figure 3(a,c), the MWDs of all the topologies with 6 or more branches/molecule were lumped together under $c \geq 6$. Similarly, in Figure 3(b,d), the mass fractions of all the topologies with 11 or more branches/molecule were lumped together under $c \geq 11$. Despite the steady reduction in the average molecular weights

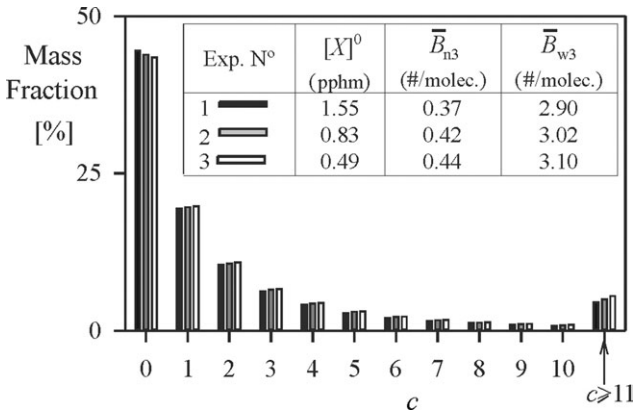

Figure 4. Model predictions for the LCBDs of Experiments 1–3 by Minari et al.[4] at 82.6% conversion. The three distributions are all quite similar, despite the relatively large variations in the initial CTA concentration ($[X]^0$).

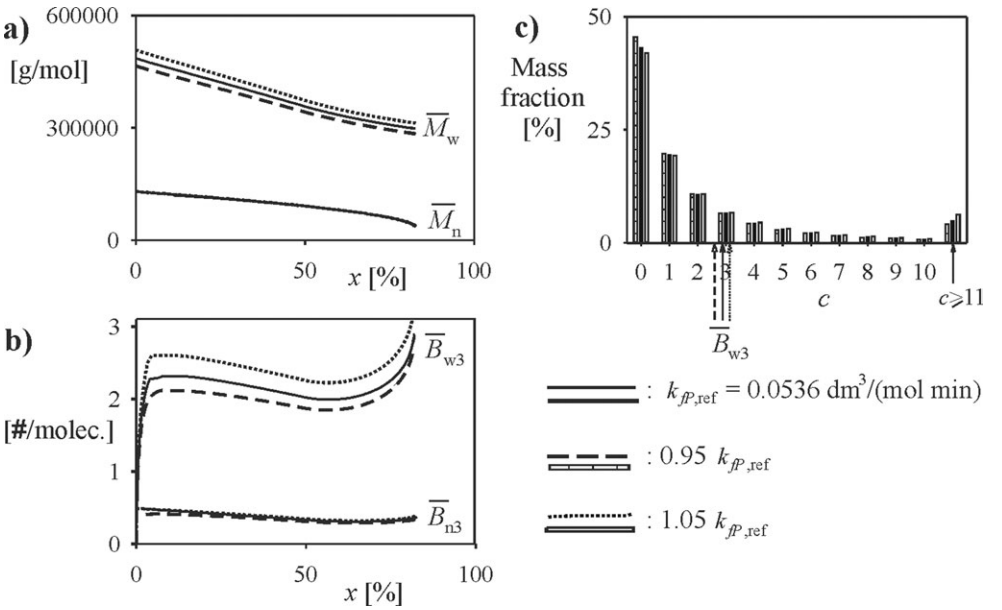

Figure 5. Sensitivity of the molecular characteristics towards ±5% variations in the rate constant of chain transfer to the polymer (k_{fP}) with respect to the reference value $k_{fP,ref}$ = 0.0536 dm³/(mol min) adopted for Experiment 1. Effects on the average molecular weights and number of branches/molecule. (a, b) Effects on the LCBDs at the final conversion, with the arrow indicating average values (c).

of the individual topologies [Figures 2(b,c) and 3(a,c)], note that the LCBD remains essentially constant along the reaction [Figure 3(b,d)].

The three experiments by Minari et al.[4] involved changes in the initial CTA concentration (from 1.55 pphm in Experiment 1, to 0.83 and 0.49 pphm in Experiment 2 and 3); while maintaining all the other conditions unmodified. As mentioned before, a diffusion control effect was imposed on the transfer to the polymer rate constant (k_{fp}) (in a reaction involving two large molecules: a macroradical and an accumulated polymer molecule).[4] More specifically, the value of k_{fp} was reduced for the increasing $\overline{M}_w$ values caused by the reduced initial CTA concentration.[4] The new model predictions (Figure 4), shows three almost coincident final LCBDs for the three simulated experiments of Minari et al.[4] This result is consistent with the insensitivity of the final $\overline{B}_{n3}$ measurements toward the initial CTA concentration.

Finally, consider the sensitivity of the molecular characteristics toward variations in k_{fP}. Figure 5 presents the effects of changing k_{fP} by ±5% with respect to the reference value of Table III, while maintaining the other parameters unmodified. Figure 5(a,b), respectively, present the evolution of the average molecular weights and average number of branches/molecules. Note that while $\overline{M}_w$ and $\overline{B}_{w3}$ are strongly affected by k_{fP}, this is not the case of $\overline{M}_n$ and $\overline{B}_{n3}$. Figure 5(c) compares the final LCBDs. When increasing k_{fP}, then the mass of linear chains is reduced, and the mass of higher topologies is increased.

CONCLUSIONS

A previous mathematical model was extended to predict the detailed branching characteristics of an emulsion polyisoprene (such detailed branching characteristics remain unclear from the single estimates of $\overline{B}_{n3}$ obtained from the base model by Minari et al.[4]).

The extended model maintains all the base assumptions of Minari et al.[4] Thus, the new model is applicable onto emulsion systems where most of the dead polymer is generated in the polymer phase by chain transfer reactions (to the CTA and to the polymer). These (rather strong) requirements have been previously applied onto other emulsion polymerizations.[7,29,30] In the investigated process, the mentioned conditions are justified because: (a) the monomer exhibits a low water solubility (and therefore a negligible amount of polymer is generated in the water phase); and (b) the number of radicals per particle is low (and therefore recombination termination between macroradicals in the polymer particles becomes negligible).

Batch emulsion polymerizations of isoprene are not commercially appealing, due to the high dispersities of the distributions of molecular weights and number of branches/molecules. However, such distributions could be conveniently narrowed through appropriate semi-batch control strategies developed with the help of a representative model, such as that presented in this work.

Quantitative measurements of the LCBD are so far impossible. For this reason, theoretical estimates of such distribution based on representative polymerization models could be useful for predicting global polymer properties such as the melt viscosity (with addition of a rheological model). Another potential application of the model is the simulation of size exclusion chromatograms of long chain-branched polymers (e.g., Casis et al.[36]).

ACKNOWLEDGMENTS

The authors are grateful for the financial support received from CONICET, Universidad Nacional del Litoral, and ANPCyT (Argentina). They also thank Petrobras Energia S.A. for providing most of the reagents.

APPENDIX: MACROMOLECULAR STRUCTURE MODULE

Call C* any unreacted repeating unit in the polymer, and call $[R^{\cdot}] = \sum_c \sum_d \sum_n \sum_m [R^{\cdot}_{(n)}(m)_{c,d}]$ the global concentration of free radicals in the polymer phase. From the global kinetics of Table I, and with the pseudo-stationary state assumption, the following material balances can be written for the global concentration of free-radicals in the polymer phase:

$$\frac{d\{[R^{\cdot}]V_p\}}{dt} = \{k_{pX}[\mathrm{Is}][X^{\cdot}] - k_{fX}[X][R^{\cdot}]\}V_p \cong 0 \quad (A1)$$

$$\frac{d\{[X^{\cdot}]V_p\}}{dt} = \{k_{fX}[X][R^{\cdot}] - k_{pX}[\mathrm{Is}][X^{\cdot}]\}V_p \cong 0 \quad (A2)$$

where V_p is the polymer phase volume.

From the detailed kinetics of Table IV, the molar balances for every possible radical species provide:

$$\frac{d([R^{\cdot}_{(1)}(0)_{0,0}]V_p)}{dt} = \{k_{pX}[\mathrm{Is}][X^{\cdot}] + k_{fM}[\mathrm{Is}][R^{\cdot}] - (k_p[\mathrm{Is}] + k_{fM}[\mathrm{Is}] + k_{fX}[X] + k_{fP}[C^*] + k_p^*[C^*])[R^{\cdot}_{(1)}(0)_{0,0}]\}V_p \quad (A3)$$

$$\frac{d([R^{\cdot}_{(n)}(0)_{0,0}]V_p)}{dt} = \{k_p[\mathrm{Is}][R^{\cdot}_{(n-1)}(0)_{0,0}] - (k_p[\mathrm{Is}] + k_{fM}[\mathrm{Is}] + k_{fX}[X] + k_{fP}[C^*] + k_p^*[C^*])[R^{\cdot}_{(n)}(0)_{0,0}]\}V_p \quad (n = 2, 3, \ldots) \quad (A4)$$

$$\frac{d([R^{\cdot}_{(0)}(m)_{a,0}]V_p)}{dt} = \{k_{fP}[P(m)_{a-1,0}]\, m\, [R^{\cdot}] - (k_p[\mathrm{Is}] + k_{fM}[\mathrm{Is}] + k_{fX}[X] + k_{fP}[C^*] + k_p^*[C^*])[R^{\cdot}_{(0)}(m)_{a,0}]\}V_p \quad (m, a = 1, 2, \ldots) \quad (A5)$$

$$\frac{d([R^{\cdot}_{(0)}(m)_{0,b}]V_p)}{dt} = \{k_p^* \sum_z [R^{\cdot}_{(z)}(0)_{0,0}][P(m-z)_{0,b-1}](m-z) + k_p^* \sum_{v=0}^{b-1} \sum_{u=1}^{m-1} [P(u)_{0,v}](u) \times \sum_w [R^{\cdot}_{(w)}(m-u-w)_{0,b-1-v}] - (k_p[\mathrm{Is}] + k_{fM}[\mathrm{Is}] + k_{fX}[X] + k_{fP}[C^*] + k_p^*[C^*])[R^{\cdot}_{(0)}(m)_{0,b}]\}V_p \quad (m, b = 1, 2, \ldots) \quad (A6)$$

$$\frac{d([R^{\cdot}_{(0)}(m)_{a,b}]V_p)}{dt} = \{k_{fP}[P(p)_{a-1,b}](p)[R^{\cdot}] + k_p^* \sum_{u=0}^{a} \sum_{v=0}^{b-1} \sum_{w=1}^{m-1} [P(w)_{u,v}] \times \sum_{z=0} [R^{\cdot}_{(z)}(m-w-z)_{a-u,b-1-u}] - (k_p[\mathrm{Is}] + k_{fM}[\mathrm{Is}] + k_{fX}[X] + k_{fP}[C^*] + k_p^*[C^*])[R^{\cdot}_{(0)}(m)_{a,b}]\}V_p \quad (m = 1, 2, \ldots); (a, b = 0, 1, 2, \ldots); (a, b \neq 0, 0) \quad (A7)$$

$$\frac{d([R^{\cdot}_{(n)}(m)_{a,b}]V_p)}{dt} = \{k_p[\mathrm{Is}][R^{\cdot}_{(n-1)}(m)_{a,b}] - (k_p[\mathrm{Is}] + k_{fM}[\mathrm{Is}] + k_{fX}[X] + k_{fP}[C^*] + k_p^*[C^*])[R^{\cdot}_{(n)}(m)_{a,b}]\}V_p \quad (m = 1, 2, \ldots); (a, b = 0, 1, 2, \ldots); (a, b \neq 0, 0) \quad (A8)$$

The weight chain length distribution (WCLD) of each (c, d) topology is obtained from a material balance for all the possible dead polymer species $P(p)_{c,d}$:

$$\frac{d([P(p)_{c,d}]V_p pM_{\mathrm{Is}})}{dt} = \{(k_{fM}[\mathrm{Is}] + k_{fX}[X] + k_{fP}[C^*]) \times \sum_n [R^{\cdot}_{(n)}(p-n)_{c,d}] - (k_{fP} + k_p^*)[P(p)_{c,d}] \times p\,[R^{\cdot}]\}V_p pM_{\mathrm{Is}} \quad (c, d = 0, 1, 2, \ldots) \quad (A9)$$

where pM_{Is} is the molecular weight of each $P(p)_{c,d}$ species.

The MWD of the total polymer is obtained by adding together eq. (A9) for all possible c's and d's, yielding:

$$\frac{d([P(p)]V_p\ pM_{\mathrm{Is}})}{dt} = \{(k_{fM}[\mathrm{Is}] + k_{fX}[X] + k_{fP}[C^*]) \times \sum_c \sum_d \sum_n [R^{\cdot}_{(n)}(p-n)_{c,d}] - (k_{fP} + k_p^*) \sum_c \sum_d [P(p)_{c,d}](p)[R^{\cdot}]\}V_p\ pM_{\mathrm{Is}} \quad (c, d = 0, 1, 2, \ldots) \quad (A10)$$

The average molecular weights of the total polymer are as follows:

$$\bar{M}_n = \frac{\sum_p \sum_c \sum_d [P(p)_{c,d}](pM_{\mathrm{Is}})}{\sum_p \sum_c \sum_d [P(p)_{c,d}]} \quad (A11)$$

$$\bar{M}_w = \frac{\sum_p \sum_c \sum_d [P(p)_{c,d}](pM_{\mathrm{Is}})^2}{\sum_p \sum_c \sum_d [P(p)_{c,d}](pM_{\mathrm{Is}})} \quad (A12)$$

The number– and weight–average numbers of trifunctional branches per molecule are as follows:

$$\bar{B}_{n3} = \frac{\sum_p \sum_c \sum_d [P(p)_{c,d}]\ c}{\sum_p \sum_c \sum_d [P(p)_{c,d}]} \quad (A13)$$

$$\bar{B}_{w3} = \frac{\sum_p \sum_c \sum_d [P(p)_{c,d}]\ (pM_{\mathrm{Is}})\ c}{\sum_p \sum_c \sum_d [P(p)_{c,d}](pM_{\mathrm{Is}})} \quad (A14)$$

REFERENCES

1. Plessis, C. Modeling of molecular weight distribution of polyacrylic latexes, Ph.D. thesis. University of the Basque Country, San Sebastian, Spain; **2000.**
2. Vittorias, I.; Parkinson, M.; Klimke, K.; Debbaut, B.; Wilhelm, M. *Rheol. Acta.* **2007,** *46*, 321.
3. Gaborieau, M.; Nicolas, J.; Save, M.; Charleux, B.; Vairon, J.-P.; Gilbert, R. G.; Castignolles, P. *J. Chrom. A.* **2008,** *1190*, 215.
4. Minari, R. J.; Rodríguez, V. I.; Estenoz, D. A.; Vega, J. R.; Meira, G. R.; Gugliotta, L. M. *J. Appl. Polym. Sci.* **2010,** *116*, 590.
5. Zubitur, M.; Ben Amor, S.; Bauer, C.; Amram, B.; Agnely, M.; Leiza, J. R.; Asua, J. M. *Chem. Eng. J.* **2004,** *98*, 183.
6. Arzamendi, G.; Sayer, C.; Zoco, N.; Asua, J. M. *Polym. React. Eng.* **1998,** *6*, 193.

7. Gugliotta, L. M.; Brandolini, M. C.; Vega, J. R.; Iturralde, E. O.; Azum, J. L.; Meira, G. R. *Polym. React. Eng.* **1995,** *3*, 201.
8. Rodríguez, V. I.; Estenoz, D. A.; Gugliotta, L. M.; Meira, G. R. *Int. J. Polym. Mater.* **2002,** *51*, 511.
9. Sweetman, S. J.; Immanuel, C. D.; Malik, T.; Emmett, S.; William, N. *Macromol. Symp.* **2006,** *243*, 159.
10. Washington, I. D.; Duever, T. A.; Penlidis, A. *J. Macromol. Sci. Part A* **2010,** *47*, 747.
11. Forcada, J.; Asua, J. M. *J. Polym. Sci. Part A: Polym. Chem.* **1990,** *28*, 987.
12. Saldivar, E.; Ray, W. H. *Ind. Eng. Chem. Res.* **1997,** *36*, 1322.
13. Plessis, C.; Arzamendi, G.; Leiza, J. R.; Schoonbrood, H. A. S.; Charmot, D.; Asua, J. M. *Ind. Eng. Chem. Res.* **2001,** *40*, 3883.
14. Zubitur, M.; Armitage, P. D.; Ben Amor, S.; Leiza, J. R.; Asua, J. M. *Polym. React. Eng.* **2003,** *11*, 627.
15. Elizalde O.; Arzamendi, G.; Leiza, J. R.; Asua, J. M. *Ind. Eng. Chem. Res.* **2004,** *43*, 7401.
16. Bouvier-Fontes, L.; Pirri, R.; Arzamendi, G.; Asua, J. M.; Leiza, J. R. *Macromol. Symp.* **2004,** *206*, 149.
17. Lichti, G.; Gilbert, R. G.; Napper, D. H. *J. Polym. Sci. Part A: Polym. Chem.* **1980,** *18*, 1297.
18. Ghielmi, A.; Fiorentino, S.; Storti, G.; Mazzotti, M.; Morbidelli, M. *J. Polym. Sci. Part A: Polym. Chem.* **1997,** *35*, 827.
19. Ghielmi, A.; Storti, G.; Morbidelli, M.; Ray, W. H. *Macromolecules* **1998,** *31*, 7172.
20. Butte, A.; Ghielmi, A.; Storti, G.; Morbidelli, M. *Macromol. Theory Simul.* **1999,** *8*, 498.
21. Prescott, S. W.; Ballard, M. J.; Gilbert, R. G. *J. Polym. Sci. Part A: Polym. Chem.* **2005,** *43*, 1076.
22. Storti, G.; Polotti, G.; Cociani, M.; Morbidelli, M. *J. Polym. Sci. Part A: Polym. Chem.* **1992,** *30*, 731.
23. Arzamendi, G.; Forcada, J.; Asua, J. M. *Macromolecules* **1994,** *27*, 6068.
24. Tobita, H.; Takada, Y.; Nomura, M. *Macromolecules* **1994,** *27*, 3804.
25. Tobita, H. *Polymer* **1994,** *35*, 3023.
26. Jabbari, E. *Polymer* **2001,** *42*, 4873.
27. Arzamendi, G.; Leiza, J. R. *Ind. Eng. Chem. Res.* **2008,** *47*, 5934.
28. Gilbert, R. G. Emulsion Polymerization: A Mechanistic Approach; Academic Press: London, **1995.**
29. Plessis, C.; Arzamendi, G.; Leiza, J. R.; Schoonbrood, H. A. S.; Charmot, D.; Asua, J. M. *Macromolecules* **2001,** *34*, 5147.
30. Minari, R. J.; Gugliotta, L. M.; Vega, J. R.; Meira, G. R. *Ind. Eng. Chem. Res.* **2006,** *45*, 245.
31. Landfester, K. *Annu. Rev. Mater. Res.* **2006,** *36*, 231.
32. Goikoetxea, M.; Minari, R. J.; Beristain, I.; Paulis, M.; Barandiaran, M. J.; Asua, J. M. *J. Polym. Sci. Part A: Polym. Chem.* **2009,** *47*, 4871.
33. Morton, M. P.; Salatiello, P. P.; Lanfield, H. *J. Polym. Sci.* **1952,** *3*, 279.
34. Estenoz, D. A.; Valdez, E.; Oliva, H.; Meira, G. R. *J. Appl. Polym. Sci.* **1996,** *59*, 861.
35. Castignolles, P.; Graf, R.; Parkinson, M.; Wilhelm, M.; Gaborieau, M. *Polymer* **2009,** *50*, 2373.
36. Casis, N.; Estenoz, D. A.; Vega, J. R.; Meira, G. R. *J. Appl. Polym. Sci.* **2009,** *111*, 1508.